C. R. Palevol 13 (2014) 41–50

Contents lists available at ScienceDirect

Comptes Rendus Palevol

www.sciencedirect.com

General palaeontology, systematics and evolution (Evolutionary processes, macroevolution)

# Theoretical morphology of tetrapod skull networks

## *Morphologie théorique de réseaux crâniens de tétrapodes*

Borja Esteve-Altava , Diego Rasskin-Gutman *

*Theoretical Biology Research Group, Institute Cavanilles for Biodiversity and Evolutionary Biology, University of Valencia, 46071 Valencia, Spain*

ARTICLE INFO

*Article history:*
Received 6 June 2013
Accepted after revision 6 August 2013
Available online 10 October 2013

Presented by Philippe Taquet

*Keywords:*
Theoretical morphology
Networks
Tetrapod skull
Evolution
Constraint
Generative morphospace
Growth rules

ABSTRACT

Network models of the tetrapod skull in which nodes represent bones and links represent sutures have recently offered new insights into the structural constraints underlying the evolutionary reduction of bone number in the tetrapod skull, known as Williston's Law. Here, we have built null network model-derived generative morphospaces of the tetrapod skull using random, preferential attachment, and geometric proximity growth rules. Our results indicate that geometric proximity is the best null model to explain the disparity of skull structures under two structural constraints: bilateral symmetry and presence of unpaired bones. The analysis of the temporal occupation of this morphospace, concomitant with Williston's Law, indicates that the tetrapod skull has followed an evolutionary path toward more constrained morphological organizations.



*Mots clés :*
Morphologie théorique
Réseaux
Crâne de tétrapode
Évolution
Contrainte
Espace morphologique génératif
Règles de croissance

RÉSUMÉ

Les modèles de réseaux crâniens dans lesquels les nœuds représentent les os et les liaisons les sutures ont récemment permis d'apporter un nouveau regard sur les contraintes structurales qui sous-tendent la réduction évolutive du nombre d'os du crâne des tétrapodes, connue sous le nom de loi de Williston. Ici ont été construits des espaces morphologiques génératifs de crânes de tétrapodes, dérivés d'un modèle de réseau nul utilisant des lois de croissance à liaison préférentielle et proximité géométrique aléatoires. Nos résultats indiquent que la proximité géométrique est le meilleur modèle nul qui permette d'expliquer la disparité des structures crâniennes sous une double contrainte : symétrie bilatérale et présence d'os non appariés. L'analyse de l'occupation temporelle de cet espace morphologique qu'explique la loi de Williston indique que le crâne de tétrapode a suivi un itinéraire évolutif vers des organisations morphologiques davantage contraintes.



## 1. Introduction

The evolution of the tetrapod skull has been extensively studied in comparative morphology. In the early 20th century, a pivotal analysis of changes in the number

* Corresponding author.
*E-mail address:* diego.rasskin@uv.es (D. Rasskin-Gutman).

1631-0683/$ – see front matter 
http://dx.doi.org/10.1016/j.crpv.2013.08.003

and complexity of skull bones in the evolution of Permian reptiles formed the basis for what is now known as the Williston's Law: an evolutionary trend in tetrapods toward reduction in the number of skull bones (Esteve-Altava et al., 2013a; Gregory, 1935; Sidor, 2001; Williston, 1914). Three complementary causal factors have been proposed to explain the reduction in the number of bones and sutures during tetrapod skull evolution (Sidor, 2001): (1) natural selection favoring more rigid, boxy skulls that improved functional and biomechanical integration in terrestrial vertebrates; (2) developmental and statistical constraints favoring the loss of bones rather than their new formation; and (3) unlikeliness of new bone formation by either genetic or epigenetic mechanisms (see also Rasskin-Gutman and Esteve-Altava, 2008 and references therein, for a review of external and internal processes related to evolutionary trends). Although reversions of Williston's Law are theoretically possible, for example, due to pedomorphosis in the patterns of cranial suture closure, this mechanism has not been reported at a broad scale as a sustained evolutionary process (but see Koyabu et al., 2011; Wilson and Sánchez-Villagra, 2009, for insights on heterochronic shifts in ossification and fusion sequences in mammals).

Recent studies on the evolution of the skull have focused on the analysis of morphological integration and modularity in different groups, such as: hominids (Bastir, 2008; Mitteroecker and Bookstein, 2009; Mitteroecker et al., 2012), mammals (Goswami, 2007; Goswami et al., 2009; Porto et al., 2009), and birds (Bhullar et al., 2012; Klingenberg and Marugán-Lobón, 2013; Marugán-Lobón and Buscalioni, 2009). In addition, the importance of cranial anatomy at all levels of organization has prompted the comparative and evolutionary analysis of gene regulatory networks (Chase et al., 2002; Haberland et al., 2009) and developmental origin of skull embryonary cells (Couly et al., 1993; Santagati and Rijli, 2003), as well as biomechanics and functional morphology (Moazen et al., 2009; Rafferty et al., 2003). These studies show that although the organization of the skull is modular at the genetic, developmental, functional, and morphological level, it still retains a tight integration of parts. As a consequence, the bony elements of the skull, which derive from multiple developmental and evolutionary origins, carry many coordinated functions (e.g., protection and hosting of sensory organs and the brain, feeding, or breathing). To which extent this multi-functional, highly integrated, and modular anatomical structure has occupied the morphospace of all possible tetrapod forms is missing in this picture. Here, we will try to answer this question duly by exploring theoretical morphospaces using network theory; with these tools we can simulate millions of networks that represent possible skulls at a broad macroevolutionary scale, using different null models of growth.

In previous works we have shown that the structure of the tetrapod skull can be efficiently analyzed using network theory (Esteve-Altava et al., 2011, 2013a, 2013b, 2013c; Rasskin-Gutman, 2003). The skull is represented as a network of bones and suture connections; this network has several mathematical properties that can be compared across taxa and during geological time. In particular, we demonstrated that Williston's Law is a trend of reduction in the number of bones that involves an increase in net structural complexity due to the random loss of poorly connected bones and the selective fusion of the most connected ones (Esteve-Altava et al., 2013a, 2013b). Here, we extend the network analysis of the tetrapod skull by merging network theory with theoretical morphology, using null network models in order to explore systematically the space of possible connections.

## 2. Theoretical morphology and networks

Theoretical morphology appeared in the 1960s beginning with the seminal work of David Raup on the accretionary growth of coiling shells (Raup, 1961, 1962, 1966, 1967, 1968). This methodological approach is based on the construction of a space of possible forms by using a set of generative rules that are formal abstractions of growth patterns (for recent extensive reviews of theoretical morphology and examples of morphospaces, see Dera et al., 2008; McGhee, 1998, 2007). An empirical morphospace including both extinct and extant forms is subsequently superimposed onto the theoretical morphospace; as a result of this mapping, real forms can be analyzed against a background of possible and impossible forms, obtaining a more general picture of how real forms are distributed in nature (Fig. 1).

The dimensions of a morphospace are timeless; this makes theoretical morphology suitable to frame evolutionary patterns of morphological change (McGhee, 1998). A theoretical morphospace describes (or puts into relation) organismal forms with one basic assumption: the morphospace is not occupied uniformly (Rasskin-Gutman and De Renzi, 2009). If the models to generate these forms are carefully chosen, distances among forms and trajectories of occupation within the theoretical morphospace will inform us about underlying causes in development and evolution (Mitteroecker and Huttegger, 2009). In theoretical morphology, the distinction between possible and impossible forms depends on which generative rule is chosen to build the theoretical morphospace. Given a set of parameters, there always will be forms that are impossible either because the generative rule cannot make them or because the combination of those parameters is meaningless. For example, if we consider, by definition, that skull networks cannot be disconnected, then any combination of parameters for each null model that would grow disconnected networks has to be treated as impossible. Also note that we do not impose functional constraints on the exploration of the skull network morphospace, this means that what is biologically possible is a subset of the formally possible, which might be further constrained by functional requirements. Moreover, the set of rules based on morphogenetic processes converts a generative morphospace in a hypothesis of developmental constraint (Rasskin-Gutman, 2003; Rasskin-Gutman and Izpisúa-Belmonte, 2004). Indeed, this is how we should look at the null models presented here.

The articulation of skull bones was first analyzed in a theoretical morphology framework in Rasskin-Gutman (2003). There, only 2D bone connectivity networks were

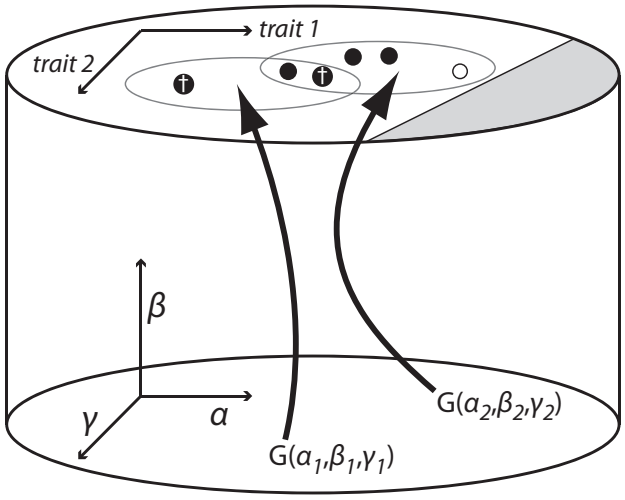


**Fig. 1.** Analysis of form using theoretical morphospaces. The empirical morphospace of morphological traits is mapped onto the broader framework provided by the theoretical construction, in which possible and impossible forms can be generated. Below, a hypothetical three-dimensional parameter space ($\alpha$, $\beta$, $\gamma$) from which a generative rule, G, explicitly builds parameter-specific regions of theoretically possible forms in the plane above. Above, the theoretical space is divided in possible regions (white) and theoretically impossible regions (grey) given the assumptions of the model. Each set of parameters for the generative rule can produce possible forms (circles), which, in the ideal case, match the empirical ones, including those that exist (solid dots), have existed in the past (crossed dots), or are functionally compromised (empty dots). Modified after Rasskin-Gutman (2005).

**Fig. 1.** Analyse de forme utilisant les espaces morphologiques théoriques. L'espace morphologique empirique des caractères morphologiques est disposé dans le cadre le plus large fourni par la construction théorique, dans laquelle les formes possibles ou impossibles peuvent être générées. En bas, espace à paramètre tridimensionnel ($\alpha$, $\beta$, $\gamma$) à partir duquel une règle générative, G, construit explicitement des régions paramétrées spécifiques, de formes théoriquement possibles dans le plan du dessus. En haut, l'espace théorique est divisé en régions possibles (en blanc) et théoriquement impossibles (en gris), étant donnés les postulats du modèle. Chaque groupe de paramètres pour la règle générative peut produire des formes possibles (cercles) qui, dans le cas idéal, correspondent aux formes empiriques comportant celles qui existent (ronds noirs) et celles qui ont existé dans le passé (ronds avec croix), ou qui sont fonctionnellement compromises (ronds blancs). Modifié d'après Rasskin-Gutman (2005).

studied from data taken from skull diagrams in lateral view. The exploration of the possible connections among skull bones was carried out using a computational model based on cellular automata, an approach that uses stochastic rules to generate connectivity patterns. These changed sequentially, following a constraint specified as a computational goal: a specific connectivity distribution and a fixed number of bones. Here, we analyze full 3D connectivity information of all bone sutures for each skull in the sample. To explore the theoretical morphospace we use null models of network growth. In general, null models are idealized representations of strategies and scenarios for a given phenomenon that also provide a comparative baseline to analyze other models (Nitecki and Hoffman, 1987). Even assuming that there is no one-to-one mapping between the network growth rule and its properties (Fox-Keller, 2005), null network models are useful heuristic tools in biology (Barabási and Albert, 1999; Watts and Strogatz, 1998). We show that the properties of these null network models, when compared with empirical skull networks reveal plausible mechanisms of network formation in evolution. Furthermore, the analysis of the growth rules and constraints that form connectivity patterns in networks can be interpreted as developmental mechanisms that impinge on skull evolutionary dynamics.

We built four null network model-derived generative morphospaces based on different growth assumptions about how bone connections are established during skull formation: at random, by preferential attachment, and using two different geometric proximity assumptions (Table 1). Each model of network growth proposes competing sets of structural constraints that might have been in place during the evolution of the tetrapod skull. The fit of skull networks to the random model would suggest absence of constraints on the formation of connections among bones. This would mean that there would be a decoupling between any evolutionary trend on skull connectivity and their underlying developmental constraints. In other words, skull connectivity trends would be exclusively due to non-developmental factors. On the other hand, the fit to the preferential attachment model would suggest that the number of connections is the main constraint in establishing new connections; thus, some bones would have a growth pattern allowing them to make contact with more and more bones as they become ossified. As far as we know, no developmental mechanism would favor this kind of preferential attachment growth. Finally, the fit to the geometric proximity models would indicate that the key factor constraining the formation of skull suture connections is the relative spatial proximity of all ossification centers. This would further suggest that changes in genetic regulatory networks that determine bone position in the developing skull (i.e., migration, determination, and differentiation of bone precursors), as well as their epigenetic regulation, could cause evolutionary changes on the formation of connections among skull bones.

We have used these four null models to build generative morphospaces, analyzing their occupation using an empirical sample of real tetrapod skull networks. The results of this approach will be used to address the following questions: (1) how does the number of connections vary in relation to the number of bones; (2) how is this variation distributed across geological time; and, most importantly, (3) which growth rules are more likely to have been involved in producing the disparity of skull structures found in nature?

## 3. Material and methods

Skull network models are a morphological abstraction of the skull suture patterns in which each bone is a node and each suture connection is a link of the network. Methods to build skull network models have been extensively discussed in Esteve-Altava et al. (2011). In the following sections, we will describe the process of construction of generative morphospaces using null network models and the empirical sample used here to analyze the morphospace occupation.

**Table 1**
Properties of the four generative morphospaces.
**Tableau 1**
Propriétés des quatre espaces morphologiques génératifs.

| Generative morphospace | Null model | Growth rule | Parameters |
|---|---|---|---|
| Random | Erdös & Rényi | Random linkage | $p = \{0.1, 0.2, 0.3\}$ |
| Preferential | Barabási & Albert | Preferential attachment | $m = \{1, 2, 3, 4, 5, 6\}$ |
| Proximal | Gabriel & Sokal | Proximity constraint | $x, y, z$ = uniformly random |
| Symmetric proximal | Gabriel & Sokal | Proximity constraint | $x$ = symmetrically random<br>$y, z$ = uniformly random |

### 3.1. Boundaries of the morphospace based on network models

We have built four generative morphospaces for two morphological traits: number of bones ($N$) and total number of suture connections between bones ($K$). These traits correspond to basic descriptors of network models: number of nodes and links. The ratio between the actual number of connections and the maximum theoretical possible, $K/N(N–1)$, defines the density of the network.

We have set the space of possible networks by imposing the following restrictions (Fig. 2): (1) redundant connections between bones, loops, are not considered (region **a** in Fig. 2), this generates an upper limit for possible theoretical networks given by a value of density = 1 (boundary **b** in Fig. 2); (2) bones cannot be disconnected (region **c** in Fig. 2), and (3) $K > N - 1$ in all instances, setting the minimum threshold of disconnectivity (boundary **d** in Fig. 2). These restrictions define the boundaries that constraint the space of modeled skull networks for all generative morphospaces (region **e** in Fig. 2).

### 3.2. Building generative morphospaces

We built four generative morphospaces: random, preferential, proximal, and symmetric proximal, using different null network models (Table 1). Each morphospace is based on a growth rule that uses different sets of parameters. Different parameter values generate different regions for each morphospace, exhibiting different degrees of overlapping. The regions generated for different values of the generative parameter delimit restricted morphospace regions, while the sum of all restricted regions configures an extended morphospace region. To set the upper and lower boundaries for each generative morphospace, the maximum and minimum values of $K$ were calculated by simulating 10,000 networks for each value of $N$, ranging from 15 to 60.

The Random morphospace is based on the classic model of Erdös and Rényi (1958), in which connections between nodes are established by random linkage. In this model, networks are built by taking a given number of nodes ($N$) and connecting each pair with probability $p$. The choice about whether or not to connect two nodes is made independently for each pair of nodes. In random networks, all connections are equally probable and there are no constraints to connectivity. Thus, the density of the generated networks depends directly on the linkage probability: if $p = 0$, the random model will generate a totally disconnected network; if $p = 1$, it will generate a complete network, where all nodes are mutually connected; and, for a large $N$ the average connectivity of the network is $p(N–1)$. In real skull networks $p$ is calculated as the ratio between the average number of connections $\bar{k}_i$ for all nodes and the total number of bones, $N$. For example, in the human skull network, $\bar{k}_i = 6.04$ and $N = 21$, so $p = 0.28$. In the empirical sample, $p$ ranges approximately from 0.1 to 0.3 (Esteve-Altava et al., 2013a); thus, we have constructed the Random morphospace for values of $p$ equal to 0.1, 0.2, and 0.3.

The preferential morphospace is based on the model proposed by Barabási and Albert (1999) to generate scale-free networks by preferential attachment. Networks are built starting from a small number of nodes (we used $N = 10$), to which new nodes are iteratively added. New nodes introduce a fixed number of new connections ($m$), connecting the new nodes to old nodes already present in the network. When choosing the old nodes to which the new node connects, those with a higher number of connections are chosen preferentially. Thus, nodes with more connections have a higher probability to attach new connections ("the rich get richer"), in contrast with the random model, in which all nodes have the same probability to connect. We have constructed the preferential morphospace for values of $m$ between 1 and 6, which cover the range of average number of connections per node in all empirical skull networks.

The Proximal morphospace is based on the model proposed by Gabriel and Sokal (1969), which imposes spatial constraints to connectivity according to node geometric proximity. Here, networks are built by positioning a given number of nodes uniformly at random in a Euclidean space; each pair of nodes is connected if, and only if, the sphere whose diameter is the line between both nodes does not have any other node within its volume. In contrast with the previous null network models, proximity networks are spatially constrained: two nodes only connect if they satisfy a geometric requirement. We have built the proximal morphospace by placing all nodes at random within a cubic space of size 1.

In addition, we have modified the model of Gabriel and Sokal to build a Symmetric Proximal morphospace, which introduces two additional constraints based on real skull anatomy: (1) the symmetric positioning of bones along a left-right axis (bilateral symmetry) and (2) the presence of unpaired bones positioned in the midline of this

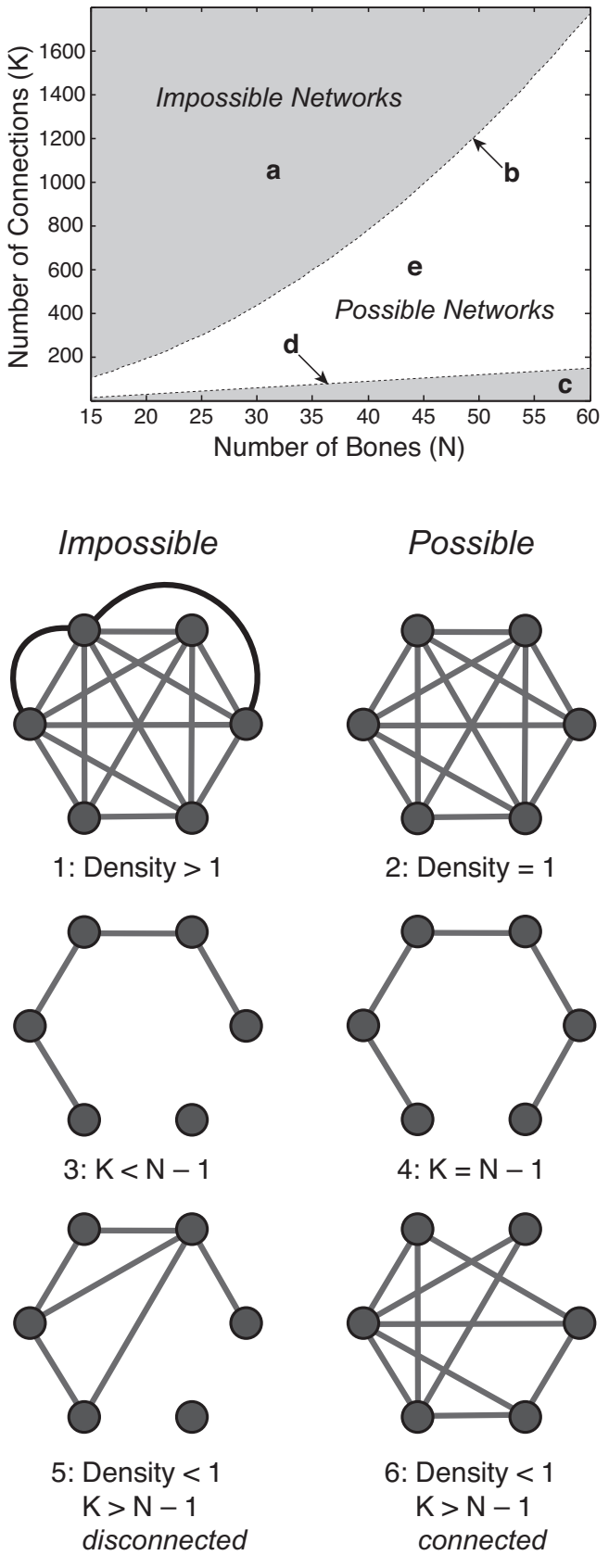


**Fig. 2.** Boundaries constraining the theoretical morphospace of skull networks. Possible skull networks occupy the white region between both boundaries, whereas the grey regions contain only impossible networks. Based on measures of density, number of connections (*K*), and number of bones (*N*), five regions **a–e** can be differentiated within the morphospace: **a** includes impossible regions with redundant connections (type 1); **b** includes possible, totally connected networks (type 2); **c** includes impossible, disconnected networks (type 3); **d** includes possible networks of minimal connectivity (type 4); and **e** includes most possible networks found in nature (type 6), but also some special impossible networks (type 5).

axis. We built the Symmetric Proximal morphospace for 0 to 7 unpaired nodes, while the remaining nodes were paired.

### 3.3. Empirical sample of skull network models

An empirical sample of 53 skull networks has been used to explore their occupation within each generative morphospace (Table 2). The sample includes 44 network models of adult tetrapod skulls (described in detail in Esteve-Altava et al., 2013a). Two basal amphibian skulls have been added to this sample: *Brachydectes* sp. (Marjanovic and Laurin, 2008) and *Pantylus* sp. (Romer, 1969). In addition, seven network models of human newborn skulls were built; the normal human skull at birth (Gray, 1918) and six nonsyndromic craniosynostosis conditions in which premature fusion of the following sutures occurs: metopic, sagittal, hemicoronal, bicoronal, lambdoidal, and lambdoidal plus occipitomastoid (Rice, 2008). The inclusion of these six pathological human skulls broadens the empirical sample with developmentally possible forms, challenging the limits of each generative morphospace. All these skulls were selected to show a wide diversity of tetrapod forms, including extinct basal forms. It is also worth noting that the identification of bones and suture connections is a very hard task in extinct species due to preservation problems in fossil skulls; in these cases, bones and connections have been quantified according to expert descriptions in the literature (as indicated in Table 1) and personal judgment.

### 3.4. Morphospace occupation

Empirical skull networks have been mapped onto each generative morphospace in order to analyze their occupation. Additionally, a temporal analysis of the morphospace occupation has been carried out for the generative morphospace that shows the best fit to the empirical sample. We have used seven time intervals: Devonian, Carboniferous, Permian, Triassic, Jurassic, Cretaceous, and Cenozoic. Temporal occupation for each empirical skull network was taken at the genus level using origin and extinction occurrence from the Paleobiological Database (available at http://paleodb.org). Extant genera without known fossil record were marked as originating in the Cenozoic.

**Fig. 2.** Liaisons contraignant l'espace morphologique théorique des réseaux crâniens. Les réseaux crâniens possibles occupent la zone blanche entre deux liaisons, tandis que les régions grises ne comportent que les réseaux impossibles. Sur la base de mesures de densité, du nombre de connexions (*K*) et d'os (*N*), cinq régions (**a**–**e**) peuvent être différenciées au sein de l'espace morphologique : **a** comporte les régions impossibles avec connexions redondantes (type 1) ; **b** comporte les réseaux possibles, totalement connectés (type 2) ; **c** comporte les réseaux impossibles, déconnectés (type 3) ; **d** comporte les réseaux possibles à connectivité minimale (type 4); **e** comporte la plupart des réseaux possibles trouvés dans la nature (type 6), mais aussi quelques réseaux spéciaux impossibles (type 5).

**Table 2**
Empirical skull network sample.
**Tableau 2**
Échantillon empirique de réseau crânien.

| Taxa | Bones (*N*) | Connections (*K*) | Period |
|---|---|---|---|
| *Anser anser*[a] | 18 | 27 | Cenozoic |
| *Brachydectes* sp.[c] | 40 | 81 | Carboniferous |
| *Canis lupus*[a] | 29 | 97 | Cenozoic |
| *Carettochelys insculpta*[a] | 36 | 92 | Cenozoic |
| *Chelodina longicollis*[a] | 33 | 80 | Cenozoic |
| *Chelydra serpentina*[a] | 36 | 91 | Cenozoic |
| *Chisternon* sp.[a] | 36 | 98 | Cenozoic |
| *Corythosaurus casuarius*[a] | 33 | 77 | Cretaceous |
| *Crocodylus moreletii*[a] | 39 | 97 | Cenozoic |
| *Didelphis virginiana*[a] | 26 | 66 | Cenozoic |
| *Dimetrodon gigas*[a] | 45 | 111 | Permian |
| *Diplometopon zarudnyi*[a] | 26 | 57 | Cenozoic |
| *Dromaeosaurus albertensis*[a] | 41 | 99 | Cretaceous |
| *Ennatosaurus tecton*[a] | 52 | 124 | Permian |
| *Epicrionops petersi*[a] | 23 | 51 | Cenozoic |
| *Gastrotheca walkeri*[a] | 22 | 43 | Cenozoic |
| *Gopherus polyphemus*[a] | 36 | 90 | Cenozoic |
| *Hemitheconyx caudicinctus*[a] | 34 | 72 | Cenozoic |
| *Homo* at birth[b] | 25 | 73 | Cenozoic |
| *Homo* CS bicoronal[d] | 23 | 68 | Cenozoic |
| *Homo* CS hemicoronal[d] | 24 | 71 | Cenozoic |
| *Homo* CS lambdoidal[d] | 20 | 70 | Cenozoic |
| *Homo* CS lambdoidalplus occipitomastoid[d] | 23 | 67 | Cenozoic |
| *Homo* CS metopic[d] | 24 | 70 | Cenozoic |
| *Homo* CS sagittal[d] | 24 | 70 | Cenozoic |
| *Homo sapiens*[a] | 21 | 64 | Cenozoic |
| *Ichthyostega* sp.[a] | 56 | 148 | Devonian |
| *Iguana iguana*[a] | 42 | 122 | Cenozoic |
| *Jonkeria ingens*[a] | 51 | 130 | Permian |
| *Kayentachelys aprix*[a] | 38 | 101 | Jurassic |
| *Mus musculus*[a] | 28 | 80 | Cenozoic |
| *Ornithorhynchus anatinus*[a] | 26 | 65 | Cenozoic |
| *Pantylus* sp.[e] | 51 | 146 | Permian |
| *Petrolacosaurus kansensis*[a] | 55 | 132 | Carboniferous |
| *Phascolarctos cinereus*[a] | 31 | 87 | Cenozoic |
| *Plateosaurus engelhardti*[a] | 49 | 112 | Triassic |
| *Podocnemis unifilis*[a] | 34 | 90 | Cenozoic |
| *Procolophon pricei*[a] | 45 | 120 | Permian-Triassic |
| *Proganochelys quenstedti*[a] | 43 | 111 | Triassic |
| *Pteropus lylei*[a] | 21 | 47 | Cenozoic |
| *Python regius*[a] | 35 | 68 | Cenozoic |
| *Rhamphorhynchus* sp.[a] | 41 | 95 | Jurassic |
| *Salamandra salamandra*[a] | 25 | 52 | Cenozoic |
| *Seymouria baylorensis*[a] | 56 | 144 | Permian |
| *Sphenodon punctatus*[a] | 38 | 78 | Cretaceous-Cenozoic |
| *Stegosaurus armatus*[a] | 47 | 114 | Jurassic |
| *Stenocercus guentheri*[a] | 44 | 97 | Cenozoic |
| *Testudo graeca*[a] | 34 | 94 | Cenozoic |
| *Thrinaxodon liorhinus*[a] | 41 | 87 | Triassic |
| *Tupinambis teguixin*[a] | 42 | 94 | Cenozoic |
| *Tursiops truncatus*[a] | 32 | 99 | Cenozoic |
| *Varanus salvator*[a] | 42 | 85 | Cenozoic |
| *Younginia capensis*[a] | 53 | 122 | Permian |

[a] Esteve-Altava et al., 2013a, 2013b, 2013c.
[b] Gray, 1918.
[c] Marjanovic and Laurin, 2008.
[d] Rice, 2008.
[e] Romer, 1969.

## 4. Results

### 4.1. Coverage of the theoretical morphospace

Generative morphospaces cover the theoretical morphospace distinctively; in addition, each type of morphospace behaves differently when varying their parameter values (Fig. 3). The random and the preferential morphospaces include all empirical networks, as parameters $p$ and $m$ vary for 0.1 to 0.3 and from 1 to 6, respectively. However, within these restricted regions some areas remain unoccupied by empirical data. In

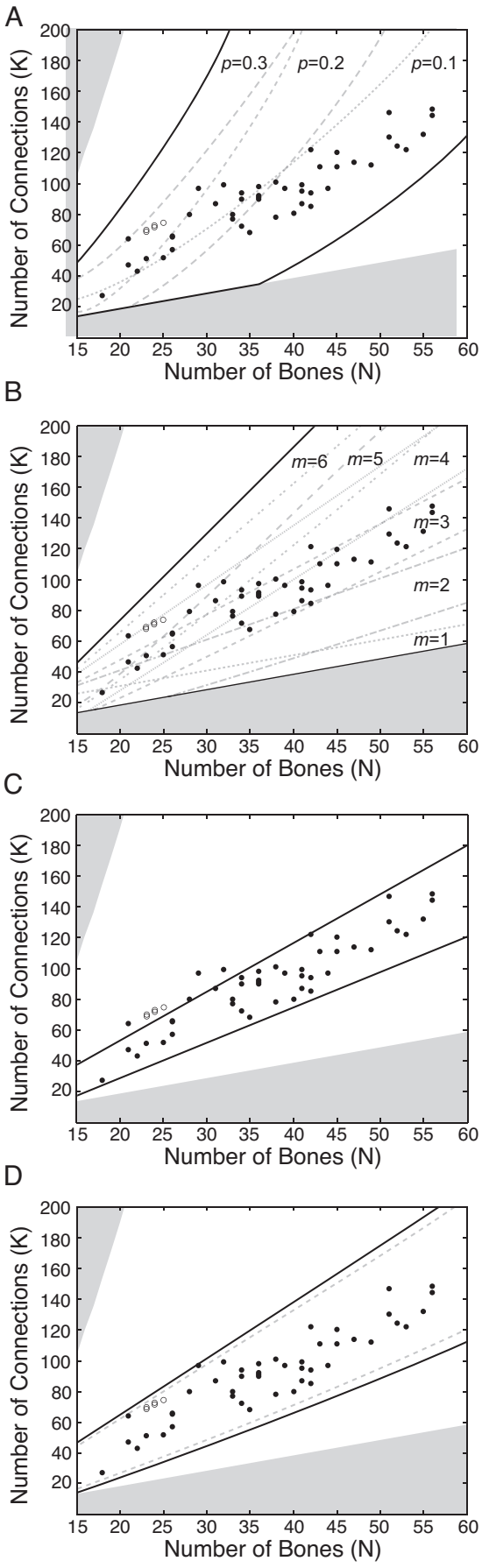


contrast, proximal morphospaces only generate networks in a limited constant region, which are almost uniformly occupied by empirical data. Note that in the case of the symmetric proximal morphospace, its form is prominently narrower for lower values of $N$ and $K$ than for higher values; consequently, the occupation is more scattered as the values of $N$ and $K$ increase.

The occupation of the Random morphospace varies in each restricted region, according to the probability value (Fig. 3A): $p = 0.1$ (58%); $p = 0.2$ (49%); and $p = 0.3$ (21%). In the Preferential morphospace, occupation also varies in each restricted region, according to the number of new connections introduced for new nodes as the network grows (Fig. 3B): $m = 1$ (2%); $m = 2$ (9%); $m = 3$ (68%); $m = 4$ (55%); $m = 5$ (26%); $m = 6$ (17%). In addition, for each set of parameters there are different areas of non-occupation; for example, for values of $p = 0.2$ and 0.3, the random morphospace is occupied by forms that are over-connected when compared with real skull networks; and for $p = 0.1$ the smaller networks generated in this morphospace are under-connected. For the preferential morphospace, most areas generated for $m = 1$, 2, 5, and 6 are empty, while the empirical sample occupies more uniformly the areas generated for $m = 3$ and 4. Finally, for $m = 1$ and 2, the generated networks are under-connected for their size, whereas for $m = 5$ and 6 the generated networks are over-connected for their size when they are compared with real skull networks.

Morphospaces generated with spatial constraints are more uniformly occupied. The proximal morphospace includes 42 out of 53 skull networks (79%) inside its boundaries (Fig. 3C); some skulls such as all human

**Fig. 3.** Coverage of the theoretical morphospace by the four generative morphospaces. In grey, the region of impossible forms; in white, the region of possible forms, which each model covers distinctively. Solid dots, adult empirical skull networks; empty dots, human newborns. For each morphospace, the regions generated for different values of the generative parameter delimit restricted morphospace regions (grey line patterns), while the sum of all restricted regions configures an extended morphospace region (black continuous lines). A. The random morphospace; forms can be generated in three restricted regions according to the probability value, $p$. B. The preferential morphospace; forms can be generated in six restricted regions according to the number of new connections introduced for new nodes as the network grows, $m$. C. The proximal morphospace; forms can be generated within a unique, uniform restricted region. D. The symmetric proximal morphospace; here the restricted and extended regions are almost identical. In all models, the distribution of $K$ for each $N$ is normal around the mean value.

**Fig. 3.** Recouvrement de l'espace morphologique théorique par quatre espaces morphologiques génératifs. En gris, la région de formes impossibles ; en blanc, la région de formes possibles que chaque modèle recouvre de manière distinctive. Points noirs, réseaux crâniens empiriques adultes ; points blancs, nouveau-nés humains. Pour chaque espace, les régions générées pour les différentes valeurs du paramètre génératif délimitent des régions réduites de l'espace morphologique (lignes grises), la somme des régions réduites configurant une région élargie de l'espace morphologique (lignes noires continues). A. Espace morphologique aléatoire ; les formes peuvent être générées dans trois régions réduites, selon la valeur de probabilité, $p$. B. Espace morphologique préférentiel ; les formes peuvent être générées dans six régions réduites, selon le nombre $m$ de nouvelles connexions introduites pour de nouveaux nœuds, quand le réseau s'accroît. C. Espace morphologique proximal ; les formes peuvent être générées au sein d'une unique région réduite uniforme. D. Espace morphologique proximal symétrique ; ici, les régions réduites et élargies sont à peu près identiques. Dans tous les modèles, la distribution de $K$ pour chaque valeur de $N$ est normale autour d'une valeur moyenne.

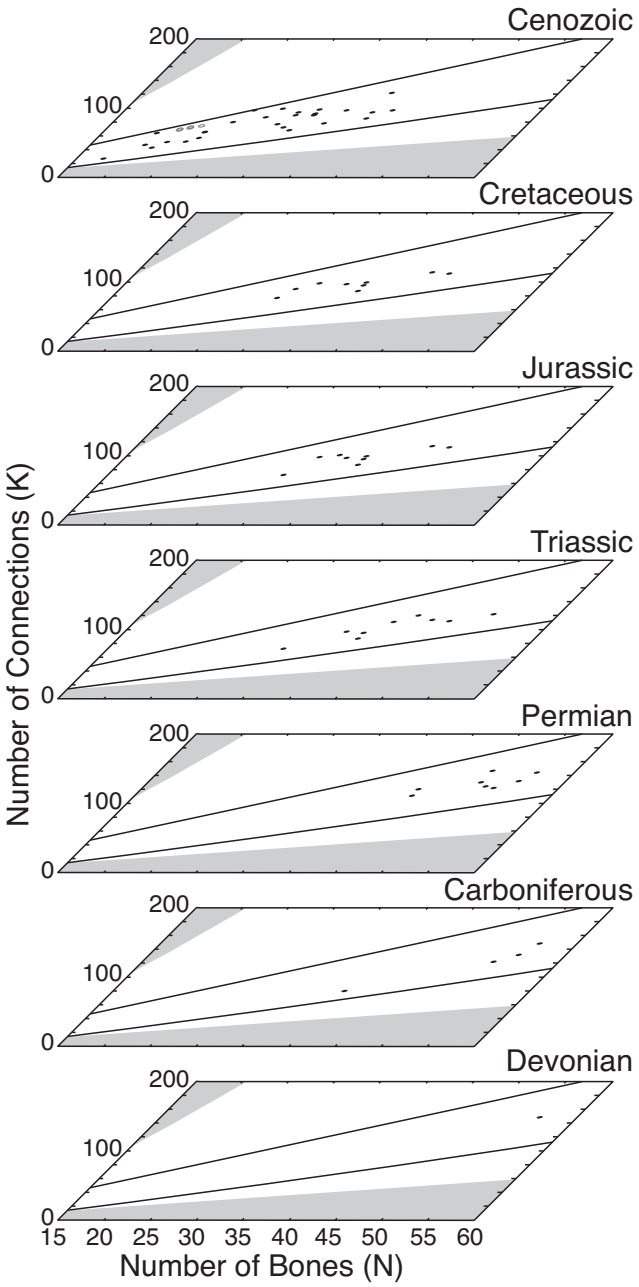


**Fig. 4.** Temporal occupation of the theoretical morphospace. Black lines delimit the area generated by the symmetric proximal morphospace. Skull networks of major groups originate in the wider area of the morphospace (right; higher *N* and *K*), in which the disparity of networks is potentially greater; after the Devonian, all groups evolved toward the narrower part of the morphospace (left; lower *N* and *K*), in which the potential disparity of skull networks is lower. By the Cenozoic, the area where skulls originated is empty.

**Fig. 4.** Occupation dans le temps de l'espace morphologique théorique. Les lignes noires délimitent la surface générée par l'espace morphologique proximal symétrique. Les réseaux crâniens des principaux groupes proviennent de la surface la plus large de l'espace morphologique (à droite, valeurs de *N* et de *K* les plus élevées), dans laquelle la disparité potentielle des réseaux est la plus grande ; après le Dévonien, tous les groupes évoluent vers la partie la plus étroite de l'espace morphologique (à gauche, valeurs de *N* et de *K* les moins élevées), dans laquelle la disparité potentielle des réseaux crâniens est la plus faible. Au Cénozoïque, la zone d'où proviennent les crânes est vide.

newborns and some modern mammals that possess a relatively high density of connections (*Homo sapiens*, *Mus musculus*, *Canis lupus*, and *Tursiops truncatus*) fall outside this morphospace. The Symmetric Proximal morphospace includes all empirical skull networks in its extended region and all but one (*Canis lupus*) in the overlap region of all its restricted regions (Fig. 3D).

### 4.2. Temporal occupation of the theoretical morphospace

To analyze the temporal occupation of the empirical sample of skull networks within the theoretical morphospace, we have used the extended symmetric proximal morphospace (Fig. 4). This generative model fits the empirical data well, including the human pathological forms. Early tetrapod skulls occupy the wider region of the morphospace during the Devonian and Carboniferous periods. Temporal occupation changes toward the narrower area of the morphospace as the wider area (i.e., higher values of *N* and *K*) begins to empty out during the Mesozoic, being completely unoccupied in the Cenozoic.

## 5. Discussion

We have built four null network model-derived generative morphospaces using three growth rules: randomness, preferential attachment, geometric proximity, and symmetric geometric proximity. By mapping an empirical sample of skull networks onto these morphospaces, we have assessed their plausibility as developmental processes involved in the formation and evolution of the tetrapod skull. Our results indicate that geometric proximity is the best model to explain the disparity of skull structures found in tetrapods. This can only happen when bones are positioned in such a way that bilateral symmetry is kept and only a few of them are unpaired, which is the case of the symmetric proximal morphospace. Further analysis of the temporal occupation of this network morphospace reveals that early skulls, for all major groups, originated in the wider area of the morphospace, in which the variability is potentially greater. Subsequently, skull networks have evolved toward the narrower area of the morphospace, in which the potential skull variability is lower. This fits Williston's Law because the wider area represents skulls with higher number of bones and connections, whereas the narrower area represents skulls with fewer bones and connections (but showing higher density or complexity).

Our results do not support random and preferential growth rules as plausible processes of skull network formation. The analysis of the occupation of these morphospaces show that: (1) different skulls need different values for basic generative parameters, which are linked to their number of bones without any developmental or phylogenetic basis; and (2) their extended regions cover the full range of possible forms, which clearly limits their explanatory power. A common characteristic of both morphospaces is that none of their restricted regions can include completely the empirical sample of skull networks; full sample inclusion occurs only when taking all extended regions. This result entails that if skull structure

(as modeled by networks) were produced by random or preferential mechanisms for establishing connections between bones, then the basic generative parameters ($p$ and $m$, respectively) would have to vary in each case to produce different skulls. Furthermore, these two models can cover the full range of possible network forms by using more values for $p$ and $m$; increasing these parameters increases the number of connections available in relation with the number of bones. Since extended regions in the random and the preferential morphospaces cover all the space of possible forms, the bounded pattern of occupation of the empirical skull networks would need additional explanation. As a consequence, the biological predictions of these models cannot be supported. This suggests that suture connection formation is constrained by specific developmental mechanisms in the tetrapod skull, coupling development with evolutionary trends (Rasskin-Gutman and Esteve-Altava, 2008). In addition, the number of connections, solely, cannot guide the establishment of new connections via specific growth patterns in the tetrapod skull.

In contrast, geometric proximity rules are well supported by our results. Even though, in these models, the positioning of bones imposes physical constraints for establishing bone connections during skull growth, they are able to generate highly bounded regions of the theoretical morphospace, which fit the empirical data very well. Thus, the proximal morphospace includes most of the real skull networks, except several skulls that have a higher number of connections (and consequently, more density) than expected for their number of bones, namely, *Homo sapiens*, *Mus musculus*, *Canis lupus*, *Tursiops truncatus*, and human newborn skulls with craniosynostosis. The addition of a bilateral symmetry constraint to the model allows the coverage of the Symmetric Proximal morphospace to include all skulls of the empirical sample.

The different occupation of the proximal and the symmetric proximal morphospaces can be better understood if we interpret nodes in growing networks as analogous to ossification centers in skulls. For these null models, this interpretation implies also an idealized mechanism of homogeneous bone growth both in speed and direction. This is so because by connecting nodes using the Gabriel & Sokal model, we are assuming that each node is a center of growth that extends spatially until it contacts another growth front. Since some empirical skulls are not included in the Proximal morphospace, this indicates that this model is unable to predict some connections between bones. These skulls deviate from the growth assumptions of this null model because some of their bones might grow in size, have more irregular shapes, or have different developmental timing (Koyabu et al., 2011; Schoch, 2006; Wilson and Sánchez-Villagra, 2009). However, all real skull networks are included in the Symmetric Proximal morphospace, in which bone position is more realistic: two sets of bones with bilateral symmetry and a few unpaired bones in the middle. This suggests that those hypothetical bones able to overcome geometric constraints in the proximal morphospace might just be unpaired bones with a privileged position that allows them to connect to many paired bones. As a consequence, the best null model to predict the formation of the skull structure is based on a mechanism by which bones establish suture connections according to their geometric distance; furthermore, the skull bilateral symmetry as well as the presence of a few unpaired bones is essential.

The generative region in the symmetric proximal morphospace is narrower for lower values of $N$ and $K$ than for higher values. Thus, it shows a variation in the range of the number of connections for skulls with lower or higher number of bones. As a consequence, there are more structural configurations of skull networks (i.e., disparity) available in the wider area of the morphospace than in the narrower area; in contrast, in the narrow area, the variability of theoretically possible skull networks is lower, that is, more constrained. Moreover, early tetrapod skulls that originated during the Devonian and Carboniferous periods only occupy the region of the morphospace characterized by a high number of bones. Throughout the Mesozoic, the occupation shifts toward narrower areas of the morphospace; that is, skulls reduce their numbers of bones, following Williston's Law. As skull bone number decreases in early tetrapod evolution, the wider area of the morphospace begins to empty out, while that narrower area begins to fill in with more derived skull forms during the Cenozoic. Thus, the occupation of the theoretical morphospace suggests that the tetrapod skull has evolved toward more constrained morphological organizations. It is worth noting also that this directional pattern of occupation is convergent in all major groups and all measures of structural complexity increase over time (Esteve-Altava et al., 2013a).

Generative morphospaces, as hypotheses of developmental constraints, have allowed us to show a directional pattern of morphospace occupation in macroevolutionary time scales, further suggesting that the tetrapod skull has evolved in most lineages under the influence of structural constraints acting on the formation of new patterns of connectivity. These structural constraints are also related with mechanisms that favor the random loss of poorly connected bones and the selective fusion of the most connected ones, incidentally increasing morphological complexity, and providing a mechanistic basis for Williston's Law (Esteve-Altava et al., 2013a, 2013b). Taken together, these results suggest an evolutionary scenario in which a structural constraint imposed by bilateral symmetry and geometric proximity between skull bones has been operating, favoring bone loss and fusion, creating highly connected unpaired bones in the midline.

## Acknowledgements

This research project was supported by grant (BFU2008-00643) from the Spanish Ministerio de Ciencia e Innovación. We are very grateful to Guillaume Dera and Nelly A. Gidaszewski and the editor, Michel Laurin for their reviews; they help improve the first version of our manuscript. We are also in debt with our colleagues Jesús Marugán-Lobón and Héctor Botella for early fruitful discussions.

## References


Barabási, A.-L., Albert, R., 1999. Emergence of scaling in random networks. Science 286, 509–512.

Bastir, M., 2008. A systems-model for the morphological analysis of integration and modularity in the human craniofacial evolution. J. Anthropol. Sci. 86, 37–58.

Bhullar, B-A.S., Marugán-Lobón, J., Racimo, F., Bever, G.S., Rowe, T.B., Norell, M.A., Abzhanov, A., 2012. Birds have paedomorphic dinosaur skulls. Nature 487, 223–226.

Chase, K., Carrier, D.R., Adler, F.R., Jarvik, T., Ostrander, E.A., Lorentzen, T.D., Lark, K.G., 2002. Genetic basis for systems of skeletal quantitative traits: principal component analysis of the canid skeleton. Proc. Natl Acad. Sci. U S A 104, 15224–15229.

Couly, G.F., Coltey, P.M., Le Douarin, N.M., 1993. The triple origin of skull in higher vertebrates: a study in quail-chick chimeras. Development 117, 409–429.

Dera, G., Eble, G.J., Neige, P., David, B., 2008. The flourishing diversity of models in theoretical morphology: from current practices to future macroevolutionary and bioenvironmental challenges. Paleobiology 34, 301–317.

Erdös, P., Rényi, A., 1958. On random graphs. Publ. Math. Debrecen 6, 290–297.

Esteve-Altava, B., Marugán-Lobón, J., Botella, H., Rasskin-Gutman, D., 2011. Network models in anatomical systems. J. Anthropol. Sci. 89, 175–184.

Esteve-Altava, B., Marugán-Lobón, J., Botella, H., Rasskin-Gutman, D., 2013a. Structural constraints in the evolution of the tetrapod skull complexity: Williston's Law revisited using network models. Evol. Biol. 40, 209–219.

Esteve-Altava, B., Marugán-Lobón, J., Botella, H., Rasskin-Gutman, D., 2013b. Random loss and selective fusion of bones originate morphological complexity trends in tetrapod skull networks. Evol. Biol., http://dx.doi.org/10.1007/s11692-013-9245-4.

Esteve-Altava, B., Marugán-Lobón, J., Bastir, M., Botella, H., Rasskin-Gutman, D., 2013c. Grist for Riedl's mill: a network model perspective on the integration and modularity of the human skull. J. Exp. Zool. (Mol. Dev. Evol.), http://dx.doi.org/10.1002/jez.b.22524.

Fox-Keller, E., 2005. Revisiting scale-free networks. BioEssays 27, 1060–1068.

Gabriel, K.R., Sokal, R.R., 1969. A new statistical approach to geographic variation analysis. Syst. Zool. 18, 259–270.

Goswami, A., 2007. Modularity and sequence heterochrony in the mammalian skull. Evol. Dev. 9, 291–299.

Goswami, A., Weisbecker, V., Sánchez-Villagra, M.R., 2009. Developmental modularity and the marsupial-placental dichotomy. J. Exp. Zool. B. Mol. Dev. Evol. 312, 186–195.

Gray, H., 1918. Anatomy of the Human Body. Lea & Febiger, Philadelphia, 1471 p.

Gregory, W.K., 1935. Williston's Law relating to the evolution of skull bones in the vertebrates. Am. J. Phys. Anthropol. 20, 123–152.

Haberland, M., Mokalled, M.H., Montgomery, R.L., 2009. Epigenetic control of skull morphogenesis by histone deacetylase 8. Gene. Dev. 23, 1625–1630.

Klingenberg, C.P., Marugán-Lobón, J., 2013. Evolutionary covariation in geometric morphometrics data: analyzing integration, modularity and allometry in a phylogenetic context. Syst. Biol. 62, 591–610.

Koyabu, D., Endo, H., Mitgutsch, C., Suwa, G., Catania, K.C., Zollikofer, C.P.E., Oda, S., Koyasu, K., Ando, M., Sánchez-Villagra, M.R., 2011. Heterochrony and developmental modularity of cranial osteogenesis in lipotyphlan mammals. EvoDevo 2, 21.

Marjanovic, D., Laurin, M., 2008. A reevaluation of the evidence supporting an unorthodox hypothesis on the origin of extant amphibians. Contrib. Zool. 77, 149–199.

Marugán-Lobón, J., Buscalioni, A., 2009. New insight on the anatomy and architecture of the avian neurocranium. Anat. Rec. 292, 364–370.

McGhee, G.R., 1998. Theoretical Morphology: the Concept and its Applications. Columbia University Press, New York, 316 p.

McGhee, G.R., 2007. The Geometry of Evolution: Adaptive Landscapes and Theoretical Morphospaces. Cambridge University Press, Cambridge, 200 p.

Mitteroecker, P., Bookstein, F., 2009. The ontogenetic trajectory of the phenotypic covariance matrix, with examples from craniofacial shape in rats and humans. Evolution 63, 727–737.

Mitteroecker, P., Huttegger, S.M., 2009. The concept of morphospaces in evolutionary and developmental biology: mathematics and metaphors. Biol. Theory 4, 54–67.

Mitteroecker, P., Gunz, P., Neubauer, S., Müller, G., 2012. How to explore morphological integration in human evolution and development? Evol. Biol. 39, 536–553.

Moazen, M., Curtis, N., O'Higgins, P., Jones, M.E.H., Evans, S.E., Fagan, M.J., 2009. Assessment of the role of sutures in a lizard skull: a computer modelling study. Proc. R. Soc. B 276, 39–46.

Nitecki, M.H., Hoffman, A., 1987. Neutral Models in Biology. Oxford University Press, New York, 166 p.

Porto, A., Oliveira, F.B., Shirai, L.T., De Conto, V., Marroig, G., 2009. The evolution of modularity in the mammalian skull I: morphological integration patterns and magnitudes. Evol. Biol. 36, 118–135.

Rafferty, K.L., Herring, S.W., Marshall, C.D., 2003. Biomechanics of the rostrum and the facial sutures. J. Morphol. 257, 33–44.

Rasskin-Gutman, D., 2003. Boundary constraints for the emergence of form. In: Müller, G., Newman, S. (Eds.), Origination of Organismal Form. MIT Press, Cambridge, pp. 305–322.

Rasskin-Gutman, D., 2005. Modularity: jumping forms within morphospace. In: Callebaut, W., Rasskin-Gutman, D. (Eds.), Modularity: Understanding the Development and Evolution of Natural Complex Systems. MIT Press, Cambridge, pp. 207–219.

Rasskin-Gutman, D., De Renzi, M. (Eds.), 2009. Pere Alberch. The Creative Trajectory of an Evo-Devo Biologist. Publicaciones de la Universidad de Valencia, Valencia, Spain.

Rasskin-Gutman, D., Esteve-Altava, B., 2008. The multiple directions of evolutionary change. BioEssays 30, 521–525.

Rasskin-Gutman, D., Izpisúa-Belmonte, J.C., 2004. Theoretical morphology of left-right asymmetries. BioEssays 26, 405–412.

Raup, D.M., 1961. The geometry of coiling in gastropods. Proc. Natl Acad. Sci. U S A 47, 602–609.

Raup, D.M., 1962. Computer as aid in describing form in gastropod shells. Science 138, 150–152.

Raup, D.M., 1966. Geometric analysis of shell coiling: general problems. J. Paleontol. 40, 1178–1190.

Raup, D.M., 1967. Geometric analysis of shell coiling: coiling in ammonoids. J. Paleontol. 41, 43–65.

Raup, D.M., 1968. Theoretical morphology of echinoid growth. J. Paleontol. 42, 50–63.

Rice, D.P., 2008. Clinical features of syndromic craniosynostosis. Front Oral Biol. 12, 91–106.

Romer, A.S., 1969. The cranial anatomy of the Permian amphibian *Pantylus*. Breviora 314, 29–38.

Santagati, F., Rijli, F.M., 2003. Cranial neural crest and the building of the vertebrate head. Nat. Rev. Neurosci. 4, 806–818.

Schoch, R.R., 2006. Skull ontogeny: developmental patterns of fishes conserved across major tetrapod clades. Evol. Dev. 8, 524–536.

Sidor, C.A., 2001. Simplification as a trend in synapsid cranial evolution. Evolution 55, 1419–1442.

Watts, D.J., Strogatz, S.H., 1998. Collective dynamics of 'small-world' networks. Nature 393, 440–442.

Williston, S.W., 1914. Water Reptiles of the Past and Present. University of Chicago Press, Chicago, 251 p.

Wilson, L.A.B., Sánchez-Villagra, M.R., 2009. Heterochrony and patterns of cranial suture closure in hystricognath rodents. J. Anat. 214, 335–339.